SERBIAN JOURNAL OF ELECTRICAL ENGINEERING
Vol. 21, No. 3, October 2024, 391-405
UDC: 669.11:[621.317.41:666.188 **DOI: https://doi.org/10.2298/SJEE2403391M**

The Effect of Structural Changes on the Functional Properties of $Fe_{65.5}Cr_4Mo_4Ga_4P_{12}C_5B_{5.5}$ Bulk Metallic Glass

Nebojša Mitrović[1], Bratislav Čukić[1], Borivoje Nedeljković[1], Aleksandra Kalezić-Glišović[1], Nina Obradović[2]

Abstract: The ferromagnetic $Fe_{65.5}Cr_4Mo_4Ga_4P_{12}C_5B_{5.5}$ bulk metallic glass rods of 1.8 mm diameter were prepared prepared by the copper-mold casting technique. As-quenched and successive furnace annealed samples were examined by thermal analysis (DTA), X-ray diffraction (XRD), thermomagnetic, coercivity, and hardness measurements. The wide supercooled liquid region ΔT_x of 57 K and reduced glass transition temperature T_{rg} of 0.57 indicate enhanced glass forming ability and high thermal stability against crystallization. After the third annealing at 673 K the most intensive stress relief is followed by an increase in the magnetic permeability of 23%, an increase in the Curie temperature (to 558 K), and an improvement in coercivity of about 40%. Coercivity abruptly increases after thermal treatment at 773 K, indicating the presence of crystalline inclusions that hinder stress relief. The XRD pattern of the rod annealed at 873 K shows several intermetallic compounds formed by crystallizing the amorphous phase, such as $B_{48}B_2C_2$, and iron-based compounds Fe_2Mo_4C and Fe_3B. The rods were explored for the increase in hardness which evolved due to stress relief and after transformation from the amorphous into crystalline phase.

Keywords: Iron-based alloys, Bulk glassy rods, Successive annealing, Magnetic permeability, Coercivity, Hardness.

1 Introduction

The improvement of a few empirical principles of synthesis of bulk metallic glasses (BMGs) and advanced methods for estimation of increased glass forming ability (GFA) has enabled the preparation of iron-based alloys with very low critical cooling rates of just a few hundred K/s [1]. The maximum casting thickness up to about (4 – 16) mm for iron-based BMGs of the amorphous alloy

[1]Faculty of Technical Sciences, Čačak, University of Kragujevac, Svetog Save 65, 32 000 Čačak, Serbia;
E-mails: nebojsa.mitrovic@ftn.kg.ac.rs; bratislav.cukic@ftn.kg.ac.rs; borivoje.nedeljkovic@ftn.kg.ac.rs; aleksandra.kalezic@ftn.kg.ac.rs
[2]Institute of Technical Sciences, Serbian Academy of Sciences, Knez Mihailova 35, 11 000 Belgrade, Serbia;
E-mail: nina.obradovic@itn.sanu.ac.rs

systems Fe-(Cr,Mo)-(C,B)-Mn [2], Fe-Cr-Mo-(Y,Ln)-C-B [3], and Fe-(Co,Cr,Mo)-(C,B)-Y [4] were successfully achieved by melting, casting, and copper mold injection methods [5, 6].

Iron-based BMGs have been the subject of scientific research due to their unique properties (chemical, physical, and structural). They have attracted commercial interest, as they are generally more profitable than other BMG alloys. Developments during the last two decades have generated many alloys of various compositions that exhibit exceptional combinations of functional properties: excellent soft magnetic properties, high strength, and hardness together with increased corrosion resistance [7 – 13].

The BMG $Fe_{65.5}Cr_4Mo_4Ga_4P_{12}C_5B_{5.5}$ alloy has been the focus of our research due to its excellent soft magnetic properties and improved mechanical properties [14 – 16] compared to other Fe-based BMG alloys. In this alloy system, the role of Mo and Cr is to increase hardness and provide high corrosion resistance, while the metalloid combination (P, C, B) facilitates amorphous structure formation [16]. Namely, iron-based BMGs usually pose low coercive field ($H_c < 100$ A/m), very high values of maximum magnetic permeability ($\mu_{rm} > 10^4$), low magnetic losses, as well as relatively high hardness of about 1042-1400 HV [17 – 19].

The structure of amorphous alloys is thermodynamically unstable and exhibits the potential for relaxation, as well as for partial or complete crystallization during heat treatment. Therefore, knowledge of the thermal stability and thermal prehistory of the alloy sample is crucial to the successful application of BMGs as multifunctional materials [20 – 22]. The structural, and therefore physical properties of ferromagnetic BMGs, are notably dependent on thermal or combined thermo-magnetic treatments which can lead to improved properties of the material, as the result of the transformation of the starting amorphous structure.

This study examines the effect of structural changes on the functional properties of $Fe_{65.5}Cr_4Mo_4Ga_4P_{12}C_5B_{5.5}$ alloy rods due to the heating runs with an increase in annealing temperature. Specifically, the objective was to evaluate the effect of successive thermal treatments on the structural relaxation, crystallization, magnetic, and mechanical features of $Fe_{65.5}Cr_4Mo_4Ga_4P_{12}C_5B_{5.5}$ BMG samples, researching for a correlation between structural changes and evolving properties of the rods.

2 Experimental

The molten $Fe_{65.5}Cr_4Mo_4Ga_4P_{12}Cr_5B_{5.5}$ alloy was cast into a copper mold under an argon protective atmosphere to prepare BMG rods with a diameter of 1.8 mm and about 70 mm in length [14, 20], as shown in Fig. 1.

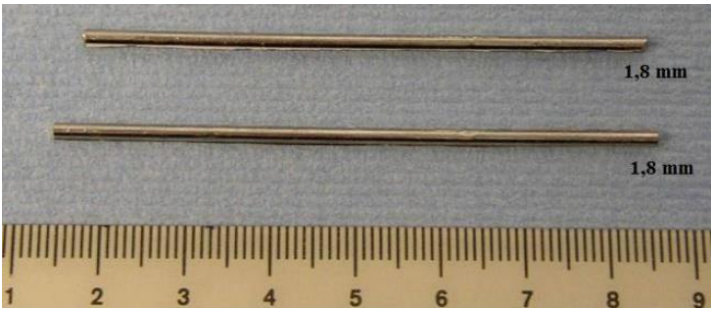

Fig. 1 – *As-cast* $Fe_{65.5}Cr_4Mo_4Ga_4P_{12}Cr_5B_{5.5}$ *BMG rods* – 1.8 mm *in diameter and about* 70 mm *in length.*

The structure of the as-cast sample and structural transformations induced by annealing were investigated by X-ray diffraction (XRD) analysis – PHILIPS PW-1050 device using Cu-Kα radiation (λ = 0.154 nm).

The thermal stability of the alloy in the temperature range between 300 K and 873 K was examined by differential thermal analysis (DTA) using a SHIMADZU 50 instrument under a protective nitrogen atmosphere.

The modified Faraday method was used for thermomagnetic measurements [23, 24]. Changes in normalized magnetic permeability in the temperature range from 300 K to 873 K, as well as resulting structural changes and increase in Curie temperature (T_c) were examined. Magnetic force during heating was measured by a SARTORIUS balance (with a sensitivity of 10^{-7} N) on samples positioned in a solenoid at the magnetic field strength of about 10 kA/m. Magnetic properties were also tested by measuring sample coercivity H_c before and after annealing using a FOERSTER coercimeter.

The rod samples were examined for microstructural changes and hardness as well. The microstructure was observed by a REICHERT POLIVAR-MET optical microscope equipped with a LEICA Q-500-MC Image Processing and Analysis System, and SEM analysis was performed by a JEOL JSM 5300 scanning electron microscope. Hardness was investigated using a REICHERT device, according to the Vickers method HV_1 (load of F = 9.81 N).

3 Results and Discussion

3.1 DTA analysis

Results of the DTA analysis of an as-prepared (non-annealed) $Fe_{65.5}Cr_4Mo_4Ga_4P_{12}C_5B_{5.5}$BMG rod sample are presented in Fig. 2. Three different events were observed: (1) ferromagnetic to paramagnetic transition denoted by Curie temperature (T_c), (2) transition from the amorphous state to the supercooled liquid state denoted by glass transition temperature (T_g) and (3)

transition to the crystalline state denoted by crystallization temperature (T_x). The Curie temperature was detected at the endothermic "λ-peak" position, T_c = 537 K. Temperatures T_g and T_x were determined as the onset of endothermic and exothermic processes, respectively, and the temperature T_p is denoted as a crystallization peak event.

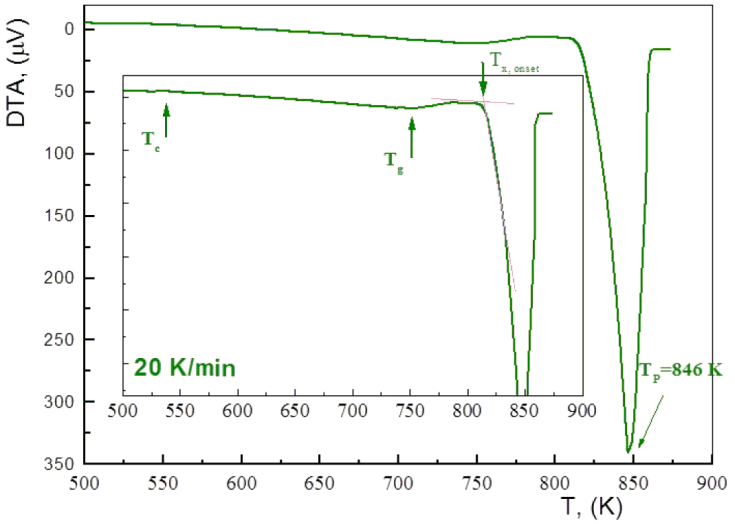

Fig. 2 – *DTA thermogram of as-prepared (non-annealed) rod of the* $Fe_{65.5}Cr_4Mo_4Ga_4P_{12}C_5B_{5.5}$ *alloy with the diameter of* 1.8 mm *(notice the wide supercooled liquid region* $\Delta T_x = T_x - T_g$ = 57 K), *heating rate* 20 K/min.

The thermogram shows that, in the temperature range between glass transition temperature, T_g and crystallization onset temperature T_x, $\Delta T_x = T_x - T_g = (810 - 753)$K, ΔT_x =57 K, the alloy exhibits a relatively wide supercooled liquid region ΔT_x followed by crystallization [11, 12, 14]. In the temperature range from 810 K to 862 K, there is a very intensive exothermic event caused by the crystallization of the alloy, with a peak temperature of T_p=846 K

The maximum diameters of the samples (d_{max}), glass transition temperatures (T_g), crystallization temperatures (T_x), supercooled liquid regions (ΔT_x), and reduced glass transition temperatures (T_{rg}) for the most common Fe-based BMG systems are given in **Table 1**.

The addition of the transition metals Hf (0-8%) [26], Ni (0-5 %) [18], and Cu (0-1%) [19] has no significant effect on the supercooled liquid region (**Table 1**). The addition of 7% Tb to the $(Fe_{72}Mo_4B_{24})_{100-x}Tb_x$ alloy (x = 4, 5, 6, 7) leads to an increase in glass transition temperature $T_g = (856 - 927)$ K [17], just as the addition of 3% Hf increase glass transition temperature $T_g = (855 - 928)$ K in the $Fe_{61}Co_6Zr_{8-x}Hf_xMo_7B_{15}Al_1Y_1$ alloy (x = 0, 3, 5, 6, 8) [26].

Table 1
Thermal properties of Fe-based BMG rods with diameters of (2 – 16) mm.

ALLOY	d_{max} (mm)	X	T_g(K)	T_x(K)	ΔT_x(K)	T_{rg}	Ref.
$(Fe_{72}Mo_4B_{24})_{100-x}Tb_x$ (x=4, 5, 6, 7)	2	4	856.0	944.0	87.9	0.62	[17]
		5	847.9	952.0	104.1	0.61	
		6	911.2	960.0	48.4	0.66	
		7	927.0	966.3	39.3	0.67	
$(Fe_{1-x}Ni_x)_{71}Mo_5P_{12}C_{10}B_2$ (x=0; 0.1 and 0.2),	3	0	731	797	66	0.58	[25]
		0.1	720	786	66	0.57	
		0.2	707	762	55	0.58	
$Fe_{61}Co_6Zr_{8-x}Hf_xMo_7B_{15}Al_1Y_1$ (x=0, 3, 5, 6, 8)	2	0	855	947	62	0.57	[26]
		3	928	978	50	0.61	
		5	918	978	60	0.60	
		8	907	968	61	0.60	
$Fe_{41}Co_{7-x}Ni_xCr_{15}Mo_{14}C_{15}B_6Y_2$ (x=0, 1, 3, 5)	3	0	846	898	52	0.58	[18]
		1	846	889	43	0.58	
		3	841	893	52	0.58	
		5	841	892	51	0.58	
$(Fe_{0.36}Co_{0.36}B_{0.192}Si_{0-048}Nb_{0.04})_{100-x}Cu_x$ (x=0; 0.5; 0.75; 1)	2	0	816	856	40	0.60	[19]
	2.5	0.5	791	830	39	0.58	
	3	0.75	767	818	51	0.56	
	2,5	1	772	815	43	0.57	
$Fe_{41}Co_7Cr_{15}Mo_{14}C_{15}B_6Y_2$	16		838	876	38	0.58	[4]
$(Fe_{44.3}Cr_5Co_5Mo_{12.8}Mn_{12.2}C_{15.8}B_{5.9})_{98.5}Y_{1.5}$	12		835.5	877	41.5	0.57	[27]

The critical diameters of the Fe-based BMG systems provided in **Table 1** are about (2 – 3) mm, except for the Y-containing alloys with rod diameters of 16 mm in $Fe_{41}Co_7Cr_{15}Mo_{14}C_{15}B_6Y_2$ [4], as well as about 12 mm in $(Fe_{44.3}Cr_5Co_5Mo_{12.8}Mn_{12.2}C_{15.8}B_{5.9})_{98.5}Y_{1.5}$ [27]. The Fe-based BMG systems listed in **Table 1** have relatively high values for reduced glass transition temperature ($0.56 < T_{rg} < 0.66$) and supercooled liquid region width (ΔT_x), thus reliably indicating the high thermal stability of the undercooled liquid. The relatively high values for reduced glass transition temperature ($T_{rg} = T_g / T_{liq} = 0.57$, $T_g = 753$ K, $T_{liq} = 1330$ K [14]) and supercooled liquid region width ($\Delta T_x = 57$ K) in $Fe_{65.5}Cr_4Mo_4Ga_4P_{12}C_5B_{5.5}$ BMG indicate good GFA and high thermal stability of the undercooled liquid relative to the process of crystallization.

The good GFA criterion implies large maximum diameters d_{max} and low critical cooling rate during melt casting. Therefore, GFA can be estimated by the mentioned temperatures T_g, T_x, and liquidus temperature T_{liq}. The investigated $Fe_{65.5}Cr_4Mo_4Ga_4P_{12}C_5B_{5.5}$ BMG alloy can be characterized by several GFA parameters: $\alpha = T_x / T_{liq} = 0.612$; $\gamma = T_x / (T_g + T_{liq}) = 0.391$; $\delta = T_x / (T_{liq} - T_g) = 1.411$. The values of these three GFA indicators are in the range of Pd-Cu-Si ($d_{max} = 2$ mm) and Mg-Ni-Nd ($d_{max} = 3.5$ mm) ternary glass-forming systems [28, 29].

3.2 XRD analysis

The XRD pattern of the as-prepared rod in Fig. 3a shows a broad maximum around $2\theta \approx 44^{O}$, i.e. an amorphous structure of 1.8 mm diameter rod is observed. The analysis of diffraction patterns presented in Fig. 3b and 3c shows that the XRD pattern of the rod sample annealed at 673 K (Fig. 3b) is quite similar to that of the as-prepared sample in Fig. 3a. As observed, there are no pronounced crystal phases and the presence of the weak boron reflections is probably due to the remaining inhomogeneity that evolved during the pre-alloy melting. Therefore, the rod sample annealed at 673 K for τ = 10 min retains its amorphous structure.

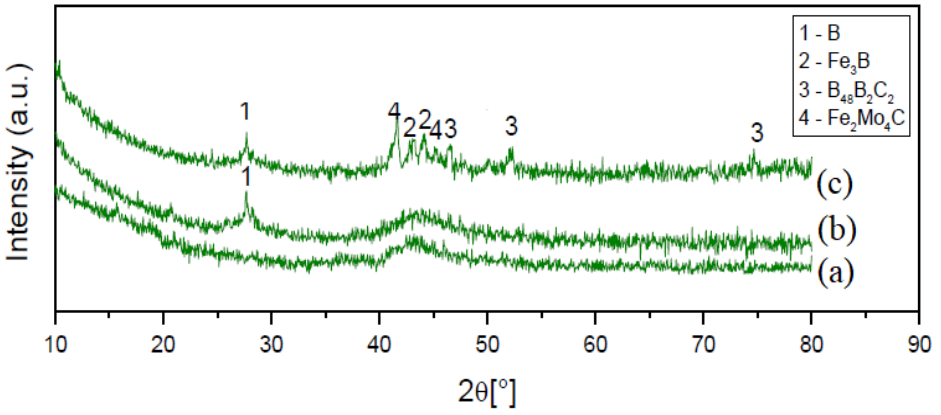

Fig. 3 – *XRD patterns of* $Fe_{65.5}Cr_4Mo_4Ga_4P_{12}C_5B_{5.5}$ BMG 1.8 mm *diameter rods:* (a) *as-prepared sample and samples annealed for* 10 min *at* (b) 673 K *and* (c) 873 K.

The comparison between the XRD patterns in Figs. 3a and 3c reveal that annealing at 873 K results in partial crystallization of the amorphous phase. The XRD pattern of the rod sample annealed at 873 K shows several diffraction peaks caused by the crystallization of the amorphous phase (Fig. 3c). Some intermetallic compounds have been formed, such as $B_{48}B_2C_2$, and iron-based compounds Fe_2Mo_4C and Fe_3B. This behavior is typical of iron-based BMGs which undergo intensive crystallization during annealing in the region near crystallization temperature, resulting in numerous intermetallic compounds [10, 11, 14].

3.3. SEM analysis

The results of the SEM analysis of the $Fe_{65.5}Cr_4Mo_4Ga_4P_{12}C_5B_{5.5}$ BMG sample are presented in Figs. 4. and 5. As shown by analysis of SEM images, upon annealing at 773 K, the amorphous matrix of the sample undergoes partial crystallization, resulting in the evolution of a large number of grains about (0.5 –1.5) μm and several irregularly shaped grains (2 – 5) μm in size (Fig. 4b).

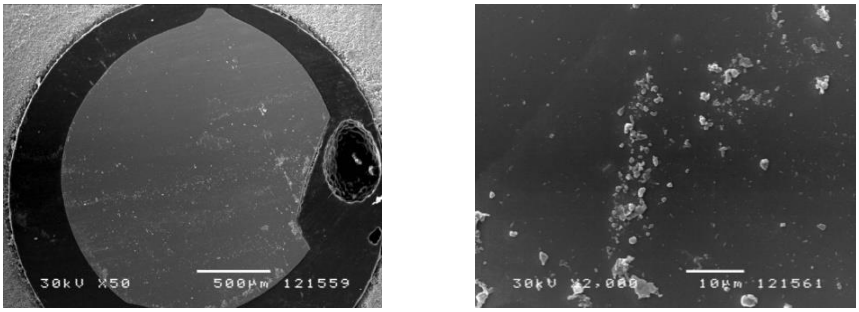

(a) (b)

Fig. 4 – *SEM images of a* 1.8 mm-*diameter rod of* $Fe_{65.5}Cr_4Mo_4Ga_4P_{12}C_5B_{5.5}$ *BMG annealed at* 773 K: (a) *the whole cross-section, and* (b) *part of the crystallized microstructure.*

The rod sample annealed at 873 K shows intensive crystallization in the amorphous matrix through the formation of a large number of homogenously distributed grains mostly spherical in shape with a size of (0.15 – 0.75) μm, and several irregularly shaped grains sized (1.5 – 3.5) μm (Fig. 5b).

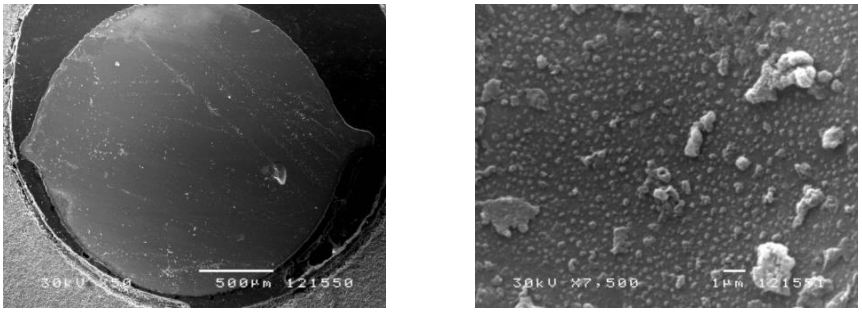

(a) (b)

Fig. 5 – *SEM images of a* 1.8 mm-*diameter rod of* $Fe_{65.5}Cr_4Mo_4Ga_4P_{12}C_5B_{5.5}$ *BMG annealed at* 873 K: (a) *the whole cross-section, and* (b) *part of the crystallized microstructure.*

The analysis of the SEM images shows intensive crystallization of the amorphous matrix after annealing. This is in agreement with the XRD results (Fig. 3c), with a set of diffraction peaks attributed to Fe_3B, $B_{48}B_2C_2$, and Fe_2Mo_4C resulting from crystallization. The wide distribution of grain shapes and sizes complies with the microstructures of other iron-based BMGs [20, 30, 31].

3.4. Thermomagnetic analysis

The results of thermomagnetic measurements after the first annealing at a temperature of 473 K, exhibit that the magnetic permeability of the sample cooled to the room temperature remains unchanged, i.e. there are no structural changes that induce changes in magnetic permeability (therefore μ_n - normalized magnetic permeability defined as μ (473 K) / μ (293 K) = μ_n (473 K) ≈ 1). The diagrams in Fig. 6 show the temperature dependence of normalized magnetic permeability of $Fe_{65.5}Cr_4Mo_4Ga_4P_{12}C_5B_{5.5}$ BMG rod sample after successive annealing at 573 K (second), and 673 K (third) for 10 min. Structural relaxation leads to the annihilation of mechanical microstrains and structural defects, and therefore there is a partially relaxed amorphous structure. The magnetic structure is with the improved mobility of the magnetic domain walls, and enhancing magnetization orientation in the external magnetic field. Therefore, an increase in the permeability of the cooled sample after the second annealing at 573 K up to 110% was observed compared to the initial as-cast structure (Figs. 6a and 8). Also, structural relaxation causes a slight change in Curie temperature, from 543 K to 553 K, Fig. 9, (I-II). After the third annealing at 673 K more intensive structural relaxation is followed by the next increase in the permeability of the cooled sample of 123% (Figs. 6b and 8), as well as the next change in Curie temperature to 558 K, Fig. 9, (III).

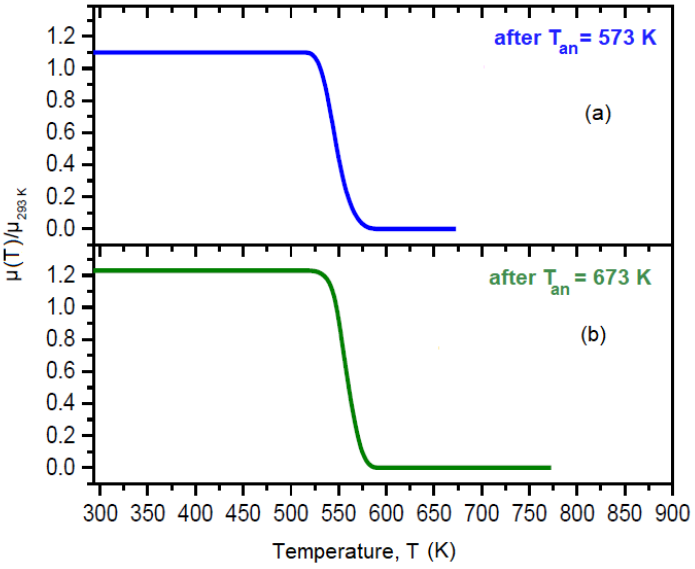

Fig. 6 – *Normalized magnetic permeability of* $Fe_{65.5}Cr_4Mo_4Ga_4P_{12}C_5B_{5.5}$ *BMG* 1.8 mm *diameter rod sample vs. temperature after successive annealing for 10 min at* (a) 573 K, *and* (b) 673 K.

The diagrams in Fig. 7 show the temperature dependence of normalized magnetic permeability of $Fe_{65.5}Cr_4Mo_4Ga_4P_{12}C_5B_{5.5}$ BMG rod sample after the next two successive annealing at 773 K (fourth), and 873 K (fifth) for 10 min. During the heating up to 873 K, the magnetic permeability remains constant up to Curie temperature, but the permeability of the cooled sample after the annealing at 773 K is about 23% lower (Figs. 7a and 8) than the maximum permeability achieved after the annealing at 673 K. This decrease in permeability after the fourth annealing at 773 K is due to grain nucleation. This trend of deterioration of soft magnetism after the annealing at 873 K is due to the onset of crystallization evidenced by evolved intermetallic compounds and Fe-based compounds according to the presented XRD pattern in Fig. 3c.

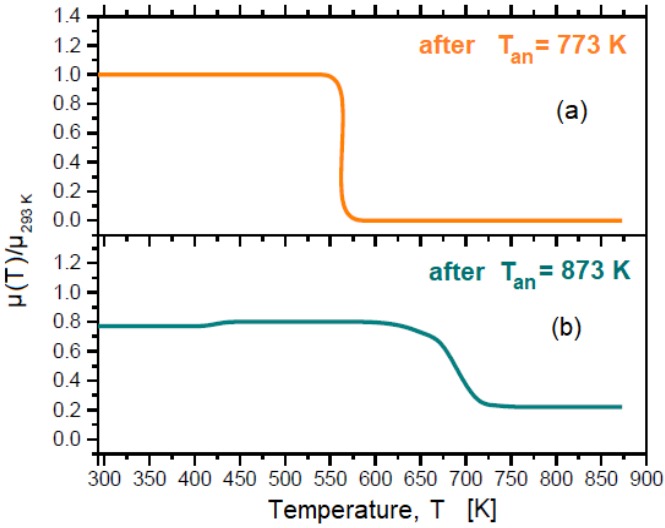

Fig. 7 – *Normalized magnetic permeability of* $Fe_{65.5}Cr_4Mo_4Ga_4P_{12}C_5B_{5.5}$ *BMG* 1.8 mm *diameter rod sample vs. temperature after successive annealing for 10 min at* (a) 773 K *and* (b) 873 K.

The crystal grains act as pinning centers for the movement of the magnetic domain walls and permeability decreases (μ_n (873 K) ≈ 0.78) as a result of magnetic hardening [32]. Therefore, upon crystallization and evolution of new compounds, a very high increment in the Curie temperature to 713 K on Fig. 9, (V) and a significant decrease in magnetic permeability occur (Figs. 7b and 8).

However, after annealing the sample at a temperature of 773 K, an increase in the normalized coercivity $H_{c,nor}$ was observed, even by about 30 times. The nucleation process and the evolution of crystal grains cause an increase in the coercivity, which follows the results of the previous research on the magnetic properties of the (Fe,Nb)-(Al,Ga)-(P,C,B) BMG system [32]. Namely, the grains

act as centers of pinning of magnetic domains and, by making the process of magnetization more difficult, lead to deterioration of soft magnetic properties [14, 32]. The increase of the annealing temperature up to the 873 K is followed by a further increase of coercivity ($H_{c,nor} \approx 55$) due to the simultaneous precipitation of several compounds upon crystalization with more intensive diffraction peaks as it is observed from the XRD pattern on Fig. 3c.

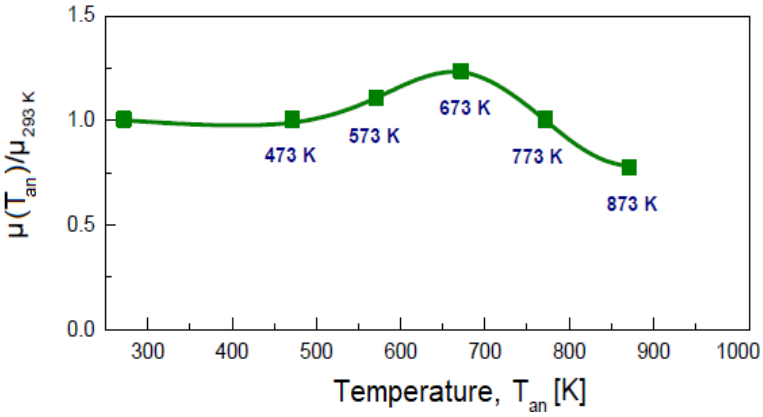

Fig. 8 – *Normalized magnetic permeability vs. annealing temperature of* $Fe_{65.5}Cr_4Mo_4Ga_4P_{12}C_5B_{5.5}$ *BMG* 1.8 mm *diameter rod sample after successive thermal treatments.*

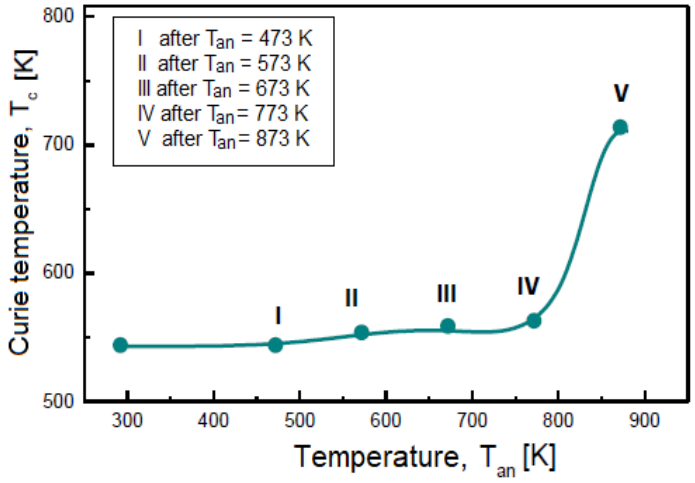

Fig. 9 – *Curie temperature vs. annealing temperature of* $Fe_{65.5}Cr_4Mo_4Ga_4P_{12}C_5B_{5.5}$ *BMG* 1.8 mm *diameter rod sample after successive thermal treatments.*

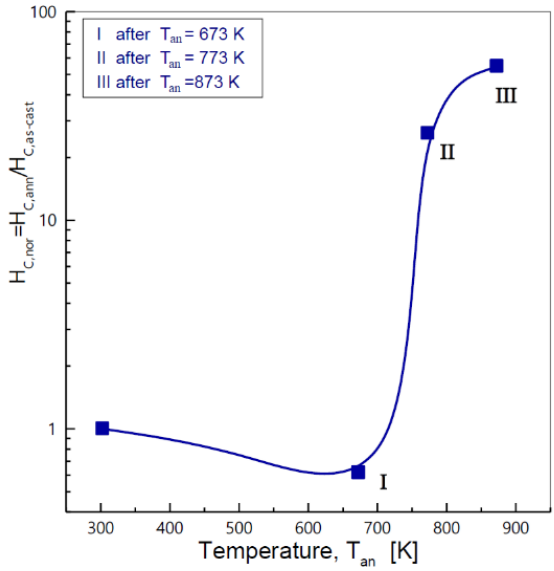

Fig. 10 – *The normalized coercivity vs. annealing temperature of* $Fe_{65.5}Cr_4Mo_4Ga_4P_{12}C_5B_{5.5}$ *BMG* 1.8 mm *diameter rod sample after successive thermal treatments.*

3.5. Structural and mechanical analyses

Fig. 11 shows the microstructures and hardness HV_1 testing of the $Fe_{65.5}Cr_4Mo_4Ga_4P_{12}C_5B_{5.5}$ BMG sample before, and after annealing (773 K and 948 K). In the as-cast sample, hardness was about $HV_1 = 713$ (Fig. 11a). Upon annealing the microstructure shows the transformation from amorphous (pristine sample) to microcrystalline (annealed) structure. The first event of nucleation, shown in Fig. 11b, was noticed after the fourth annealing at 773 K.

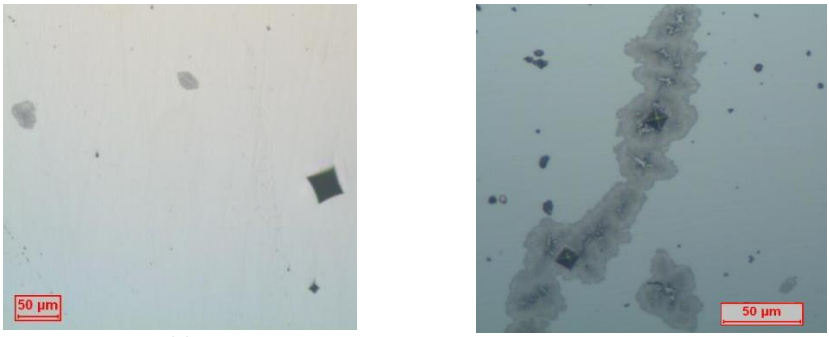

(a) (b)

Fig. 11 – *Microstructures and hardness testing of* Fe65.5Cr4Mo4Ga4P12C5B5.5 *BMG* 1.8 mm *diameter rod sample: (*a) *as-cast, and* (b) *annealed at* 773 K.

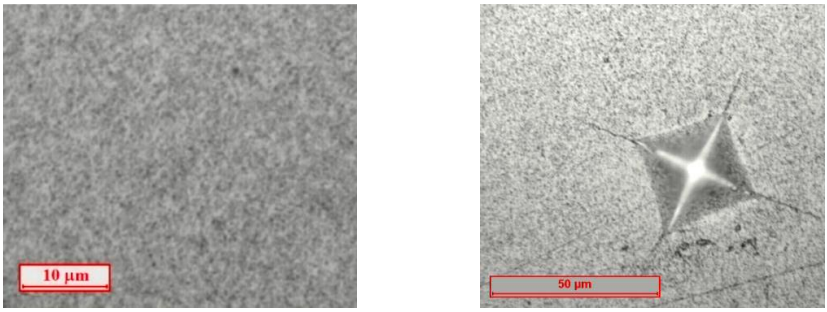

(a) (b)

Fig. 12 – *Microstructures* (a) *and hardness testing* (b) *of* $Fe_{65.5}Cr_4Mo_4Ga_4P_{12}C_5B_{5.5}$ *BMG* 1.8 mm *diameter rod sample annealed at* 948 K.

The microcrystalline structure presented in Fig. 12a and 12b is homogenous over the whole sample surface, and the crystallization process at 948 K is accompanied by an increase in hardness up to about $HV_1 = 1086$.

4 Conclusion

In this paper, structural, magnetic, and mechanical properties of the ferromagnetic $Fe_{65.5}Cr_4Mo_4Ga_4P_{12}C_5B_{5.5}$ BMG rods of 1.8 mm diameter obtained by copper mold casting were investigated.

DTA analysis showed that the alloy exhibits the features of supercooled liquids over a wide range of temperatures ($\Delta T_x = T_x - T_g = 57$ K). Moreover, crystallization was observed to occur in the temperature range of 810 K to 860 K, with the exomaximum peak at 846 K. XRD analysis revealed an amorphous structure of the 1.8 mm diameter $Fe_{65.5}Cr_4Mo_4Ga_4P_{12}Cr_5B_{5.5}$ BMG sample. The same method has detected the change in structure from amorphous to microcrystalline induced by annealing.

The increase in permeability of the cooled sample after successive annealing runs compared to the initial as-prepared rod was examined. After the third annealing at 673 K, the most intensive structural relaxation is followed by an improvement in permeability of 123%, as well as an increase in Curie temperature from 537 K to 558 K. The analysis of the effect of annealing on coercive field values showed that annealing below the crystallization temperature improved $H_{c,nor.}$, which increased after the onset of the crystallization process.

The transformation of the structure from the starting amorphous to the resulting microcrystalline state was observed by SEM and microstructural analyses. It was found that crystallization was accompanied by an increase in hardness from about HV1 = 713 in the amorphous state to about HV1 = 1086 in the microcrystalline state.

5 Acknowledgments

This research is supported in part by the Ministry of Science, Technological Development and Innovation of the Republic of Serbia, within the institutional financing, contract number 451-03-66/2024-03/200132 with the Faculty of Technical Sciences Čačak - University of Kragujevac.

6 References

[1] C. Suryanarayana, A. Inoue: Iron-based Bulk Metallic Glasses, International Materials Reviews, Vol. 58, No. 3, November, 2013, pp. 131 – 166.

[2] V. Ponnambalam, S. J. Poon, G. J. Shiflet, V. M. Keppens, R. Taylor, G. Petculescu: Synthesis of Bulk Metallic Glasses as Nonferromagnetic Amorphous Steel Alloys, Applied Physics Letter, Vol. 83, No. 6, August, 2003, pp. 1131 – 1133.

[3] V. Ponnambalam, S. J. Poon, G. J. Shiflet: Fe-based Bulk Metallic Glasses with Diameter Thickness Larger than One Centimeter, Journal of Materials Research, Vol.19, May, 2004, pp. 1320 – 1323.

[4] J. Shen, Q. J. Chen, J. F. Sun, H. B. Fan, G. Wang: Exceptionally High Glass-forming Ability of an FeCoCrMoCBY Alloy, Applied Physics Letters, Vol. 86, No. 15, May, 2005, pp. 151907-1 – 151907-3.

[5] L. Yuan, G. Jing, J. Jun: Equivalent heat transfer coefficient at casting/Cu mould interface and temperature field simulation, Transactions of Nonferrous Metals Society of China, Vol. 13, No. 5, pp. 1119 – 1123, 2003.

[6] T. Koziel, P. Matusiewicz, M. Kopyscianski, A. Z. Lipiec: Estimation of the Cooling Rate in 3 mm Suction-cast Rods Based on the Microstructural Features, Metallurgy and Foundry Engineering, Vol. 39, No. 2, January, 2013, pp. 7 – 14.

[7] T. D. Shen, R. B. Schwartz: Bulk Ferromagnetic Glasses Prepared by Flux Melting and Water Quenching", Applied Physics Letters, Vol. 75, No. 1, July, 1999, pp. 49 – 51.

[8] S. Pang, T. Zhang, K. Asami, A. Inoue: New Fe-Cr-Mo-(Nb, Ta)-C-B Glassy Alloys with High Glass-forming Ability and Good Corrosion Resistance, Materials Transaction, Vol. 42, No. 2, February, 2001, pp. 376 – 379.

[9] K. Amiya, A. Inoue: Fe-(Cr, Mo)-(C, B)-Tm Bulk Metallic Glasses with High Strength and High Glass-forming Ability, Materials Transaction, Vol. 47, No. 6, June, 2006, pp. 1615 – 1618.

[10] H. X. Li, S. L. Wang, S. Yi, Z. B. Jiao, Y. Wu, Z. P. Lu: Glass Formation and Magnetic Properties of Fe-C-Si-B-P-(Cr-Al-Co) Bulk Metallic Glasses Fabricated Using Industrial Raw Materials, Journal of Magnetism and Magnetic Materials, Vol. 321, No. 18, September, 2009, pp. 2833 – 2837.

[11] J. Zhang, W. Wang, G. Li, H. Ma, J. Qin, X. Bian: Correlation Between Microstructure and Thermal Dilation Behavior of Amorphous Fe-Co-Zr-Mo-W-B Alloys, Transactions of Nonferrous Metals Society of China, vol. 20, No. 1, January, 2010, pp.71 – 77.

[12] M. S. Bakare, K. T. Voisey, K. Chokethawal, D. G. McCartney: Corrosion Behavior of Crystalline and Amorphous Forms of the Glass Forming Alloy Fe43Cr16Mo16C15B10, Journal of Alloys and Compounds, Vol. 527, June, 2012, pp. 210 – 218.

[13] M. Stoica, J. Eckert, S. Roth, Z.F. Zhang, L. Schultz, W. H. Wang: Mechanical Behavior of Fe65.5Cr4Mo4Ga4P12C5B5.5 Bulk Metallic Glass, Intermetallics, Vol. 13, No. 7, July, 2005, pp. 764 – 769.

[14] N. Mitrović, S. Roth, M. Stoica: Magnetic Softening of Bulk Amorphous FeCrMoGaPCB Rods by Current Annealing Technique, Journal of Alloys and Compounds, Vol. 434-435, May, 2007, pp. 618 – 622.

[15] B. Čukić, N. Mitrović, A. Maričić: Effect of Heat Treatment on Structure and Magnetic Properties of Fe65.5Cr4Mo4Ga4P12C5B5.5 Bulk Amorphous Alloy, China Foundry, Vol. 14, No. 1, January 2017, pp. 59 – 63.

[16] N. Mitrović, B. Čukić, B. Jordović, S. Roth, M. Stoica: Microstructure and Microhardness in Current Annealed Fe65.5Cr4Mo4Ga4P12C5B5.5 Bulk Metallic Glass, Material Science Forum, Vol. 555, September, 2007, pp. 521 – 526.

[17] H. Jian, W. Luo, Sh. Tao, M. Yan: Mechanical and Magnetic Properties of (Fe72Mo4B24)100-xTbx (x=4, 5, 6, 7 at. %) Bulk Glassy Alloy, Journal of Alloys and Compounds, Vol. 505, No. 1, August, 2010, pp. 315 – 318.

[18] J. Han, C. Wang, S. Kou, X. Liu: Thermal Stability, Crystallization Behavior, Vickers Hardness and Magnetic Properties of Fe-Co-Ni-Cr-Mo-C-B-Y Bulk Metallic Glasses, Transactions of Nonferrous Metals Society of China, Vol. 23, No. 1, January 2013, pp. 148 – 155.

[19] M. Aykol, M. V. Akdeniz, A. O. Mekhrabov: Solidification Behavior, Glass Forming Ability and Thermal Characteristics of Soft Magnetic Fe-Co-B-Si-Nb-Cu Bulk Amorphous Alloys, Intermetallics, Vol. 19, No. 9, September, 2011, pp. 1330 – 1337.

[20] M. Stoica, J. Eckert, S. Roth, L. Schultz, A. R. Yavari, A. Kvick: Casting and Phase Transformations of Fe65.5Cr4Mo4Ga4P12C5B5.5 Bulk Metallic Glass, Journal of Metastable and Nanocrystalline Materials, Vol. 12, July, 2002, pp. 77 – 84.

[21] M. Stoica, J. Degmova, S. Roth, J. Eckert, H. Grahl, L. Schultz, A.R. Yavari, A. Kvick, G. Heunen: Magnetic Properties and Phase Transformations of Bulk Amorphous Fe-based Alloys Obtained by Different Techniques, Materials Transaction, vol. 43, No. 8, September, 2002, pp. 1966 – 1973.

[22] M. Stoica, R. Li, A.R. Yavari, G. Vaughan, J. Eckert, N.V. Steenberge, D.R. Romera: Thermal Stability and Magnetic Properties of FeCoBSiNb Bulk Metallic Glasses, Journal of Alloys and Compounds, Vol. 504S, August, 2010, pp. S123 – S128.

[23] S. Djukić, V. Maričić, A. Kalezić-Glišović, L. Ribić-Zelenović, S. Randjić, N. Mitrović, N. Obradović: The Effect of Temperature and Frequency on Magnetic Properties of the Fe81B13Si4C2 Amorphous Alloy, Science of Sintering, Vol. 43, No. 2, 2011, pp. 175 – 182.

[24] A. S. Kalezić-Glisović, L. Novaković, A. M. Maričić, D. M. Minić, N. S. Mitrović: Investigation of Structural Relaxation, Crystallization Process and Magnetic Properties of the Fe–Ni–Si–B–C Amorphous Alloy, Materials Science and Engineering B, Vol. 131, No. 1-3, July, 2006, pp. 45 – 48.

[25] S. F. Guo, N. Li, C. Zhang, L. Liu: Enhancement of Plasticity of Fe-based Bulk Metallic Glass by Ni Substitution for Fe, Journal of Alloys and Compounds, Vol. 504S, August, 2010, pp. S78 – S81.

[26] S. F. Guo, Y. Y. Sun, J. Pan, L. Liu: The Effect of Hf Substitution for Zr on Glass Forming Ability and Magnetic Property of FeCoZrMoBAlY Bulk Metallic Glasses, Journal of Alloys and Compounds, Vol. 458, No. 1-2, June, 2008, pp. 214 – 217.

[27] Z. P. Lu, C. T. Liu, J. R. Thompson, W. D. Porter: Structural Amorphous Steels, Physical Review Letters, Vol. 92, No.24, June, 2004, pp. 245503-1 – 245503-4.

[28] A. Inoue, F. L. Kong, Q. K. Man, B. L. Shen, R. W. Li, F. Al-Marzouki: Development and Applications of Fe- and Co-Based Bulk Glassy Alloys and Their Prospects, Journal of Alloys and Compounds, Vol. 615, No. Suppl. 1, December, 2014, pp. S2 – S8.

[29] C. Chattopadhyay, K. S. N. Satish Idury, J. Bhatt, K. Mondal, B. S. Murty: Critical Evaluation of Glass Forming Ability Criteria, Materials Science and Technology, Vol. 32, No. 4, April, 2016, pp. 380 – 400.

[30] K. Werniewicz, U. Kuhn, N. Mattern, B. Bartusch, J. Eckert, J. Das, L. Schultz, T. Kulik: New Fe-Cr-Mo-Ga-C Composites with High Compressive Strength and Large Plasticity, Acta Materialia, Vol. 55, No. 10, June, 2007, pp. 3513 – 3520.

[31] H. X. Li, Z. C. Lu, S. L. Wang, Y. Wu, Z. P. Lu: Fe-based Bulk Metallic Glasses: Glass Formation, Fabrication, Properties and Applications, Progress in Materials Science, Vol. 103, June, 2019, pp. 235 – 318.

[32] N. Mitrović, S. Roth, J. Eckert, C. Mickel: Microstructure Evolution and Soft Magnetic Properties of Fe72−xNbxAl5Ga2P11C6B4 (x = 0, 2) Metallic Gndlasses, Journal of Physics D: Applied Physics, Vol. 35, No. 18, September 2002, pp. 2247 – 2253.